Subcapsular sinus macrophages prevent CNS invasion on peripheral infection with a neurotropic virus

Matteo Iannacone[1,2]*, E. Ashley Moseman[1]*, Elena Tonti[1], Lidia Bosurgi[1], Tobias Junt[3], Sarah E. Henrickson[1], Sean P. Whelan[4], Luca G. Guidotti[2] & Ulrich H. von Andrian[1]

Lymph nodes (LNs) capture microorganisms that breach the body's external barriers and enter draining lymphatics, limiting the systemic spread of pathogens[1]. Recent work has shown that $CD11b^+CD169^+$ macrophages, which populate the subcapsular sinus (SCS) of LNs, are critical for the clearance of viruses from the lymph and for initiating antiviral humoral immune responses[2–4]. Here we show, using vesicular stomatitis virus (VSV), a relative of rabies virus transmitted by insect bites, that SCS macrophages perform a third vital function: they prevent lymph-borne neurotropic viruses from infecting the central nervous system (CNS). On local depletion of LN macrophages, about 60% of mice developed ascending paralysis and died 7–10 days after subcutaneous infection with a small dose of VSV, whereas macrophage-sufficient animals remained asymptomatic and cleared the virus. VSV gained access to the nervous system through peripheral nerves in macrophage-depleted LNs. In contrast, within macrophage-sufficient LNs VSV replicated preferentially in SCS macrophages but not in adjacent nerves. Removal of SCS macrophages did not compromise adaptive immune responses against VSV, but decreased type I interferon (IFN-I) production within infected LNs. VSV-infected macrophages recruited IFN-I-producing plasmacytoid dendritic cells to the SCS and in addition were a major source of IFN-I themselves. Experiments in bone marrow chimaeric mice revealed that IFN-I must act on both haematopoietic and stromal compartments, including the intranodal nerves, to prevent lethal infection with VSV. These results identify SCS macrophages as crucial gatekeepers to the CNS that prevent fatal viral invasion of the nervous system on peripheral infection.

To explore how neurotropic viruses spread from their entry site to the CNS, we studied VSV, an arthropod-borne rhabdovirus that causes fatal paralytic disease in mammals, including mice[5]. Although numerous studies have investigated immune responses to intravenous infection with VSV[6], the immunological consequences elicited by the more natural subcutaneous route are incompletely understood. Previous work has shown that, after peripheral inoculation, VSV is captured by macrophages in draining LNs, preventing haematogenous dissemination[2]. In this study we examined whether this macrophage filter affects the ability of neurotropic viruses to access the CNS.

C57BL/6 mice were injected subcutaneously with clodronate liposomes (CLLs) into one hind footpad, which selectively eliminated $CD11b^+CD169^+$ macrophages in the draining popliteal LN but not in distal LNs or the spleen[2]. Six days later, mice were challenged in the ipsilateral or contralateral footpad with a low dose (10^4 plaque-forming units (pfu)) of VSV-Indiana. Whereas this dose was cleared by virtually all untreated and contralaterally infected mice, about 60% of CLL-treated ipsilaterally infected animals developed ascending CNS pathology starting with ipsilateral hindleg paralysis and progressing to death 7–10 days after infection (Fig. 1a). Equivalent results were obtained with Balb/c mice or VSV-New Jersey (Supplementary Fig. 1). CLL-dependent susceptibility to fatal neuropathology was a direct consequence of viral CNS invasion, because infectious virus and virus-induced pathology became detectable in the brain (Fig. 1b) and spinal cord (Supplementary Fig. 2) exclusively in symptomatic CLL-treated mice.

To confirm that CLLs promoted VSV neuroinvasion through macrophage depletion and not by other mechanisms, we sought an alternative approach to eliminate LN-resident macrophages. LN macrophages express moderate levels of CD11c (ref. 2) and are susceptible to the toxic effects of diphtheria toxin in CD11c-DTR mice[7]. Indeed, injection of diphtheria toxin into the footpad eliminated $CD169^+$ LN macrophages in the draining LN, while leaving paracortical $CD11c^+$ dendritic cells unchanged (Supplementary Fig. 3). Treatment with diphtheria toxin rendered CD11c-DTR mice susceptible to fatal infection with VSV with a clinical course and mortality that were similar to those of CLL-treated animals (Fig. 1c). These results, based on two mechanistically distinct approaches, indicate that CLL-sensitive $CD11c^+$ phagocytes are essential for neuroprotection after peripheral infection with VSV.

To pinpoint the site of viral susceptibility, we considered four candidate access routes for viral neuroinvasion after subcutaneous infection in CLL-treated mice: direct entry across the blood–brain barrier either by free circulating virions[8] or by virus-bearing migratory cells, or entry through peripheral nerves in the infected footpad and/or the draining LNs.

After subcutaneous deposition of VSV, viral particles drain rapidly to regional LNs, where macrophages capture lymph-borne virions[2]. Because CLLs eliminate this macrophage filter, infectious virions can reach the blood through efferent lymphatics[2]. However, at the low VSV dose (10^4 pfu) used here, we did not detect a 'spillover' of infectious virus in blood (Supplementary Fig. 6c). Moreover, CLL-treated animals survived intravenous injections of 10^4 pfu of VSV (Fig. 1d), which is consistent with earlier reports that the median lethal dose for intravenously injected VSV is about 10^8 pfu in C57BL/6 mice[9]. Haematogenous dissemination therefore seemed an unlikely pathway by which infectious virions could access the CNS. However, it remained theoretically possible that migratory cells infected in the hindleg acted as 'Trojan horses' by transporting VSV by means of the blood into the CNS. To distinguish between this candidate pathway and the alternative access route, peripheral nerves in the hindleg, we resected sciatic nerves in CLL-treated mice before infection with VSV. Indeed, ipsilateral denervation, but not contralateral or sham denervation, protected CLL-treated mice against neuroinvasion with

[1]Immune Disease Institute and Department of Pathology, Harvard Medical School, 77 Avenue Louis Pasteur, Boston, Massachusetts 02115, USA. [2]Department of Immunology, Infectious Diseases and Transplantation, San Raffaele Scientific Institute, Via Olgettina 58, 20132 Milan, Italy. [3]Novartis Institutes for BioMedical Research, 4002 Basel, Switzerland. [4]Department of Microbiology and Molecular Genetics, Harvard Medical School, 200 Longwood Avenue, Boston, Massachusetts 02115, USA.
*These authors contributed equally to this work.

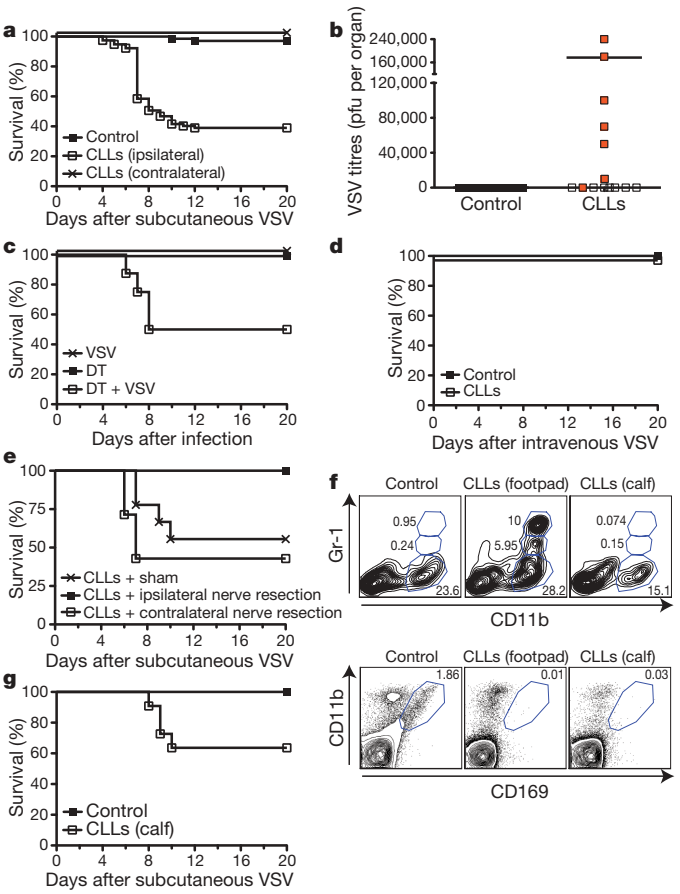

Figure 1 | Lymph node macrophages confer resistance to fatal invasion of the CNS on peripheral low-dose infection with VSV. **a**, Survival curves of control mice ($n = 68$) and mice that received ipsilateral ($n = 77$) or contralateral ($n = 10$) injection of CLLs before infection with VSV. Ipsilateral CLLs versus control, $P < 0.0001$. **b**, VSV titres in the brain of control and CLL-treated mice, 7 days after infection. Red squares identify paralytic animals. $P = 0.024$. **c**, Survival curves of CD11c-DTR mice ($n = 8$); $P = 0.0256$. **d**, Survival curves of control and CLL-treated mice after intravenous VSV infection ($n = 10$). **e**, Survival curves of CLL-treated VSV-infected mice after ipsilateral ($n = 10$) or contralateral ($n = 7$) sciatic nerve resection. $P = 0.007$. **f**, FACS plots of digested footpads (top) and the popliteal LNs (bottom) of control and CLL footpad-injected or calf-injected mice. Numbers show the percentages of $CD45^+$ cells within each gate. Plots are representative of two experiments ($n = 3$ mice per experiment). **g**, Survival curves in control ($n = 10$) and calf CLL-treated mice ($n = 11$). $P = 0.0411$.

VSV (Fig. 1e), indicating that VSV does not enter the CNS haematogenously but through distal branches of the sciatic nerve in anatomical regions that contain CLL-sensitive $CD11c^+$ phagocytes and that are directly exposed to VSV as well as CLLs; that is, the footpad and/or the draining LNs.

Because the CLL injection site developed a myeloid infiltrate during the first week (Fig. 1f), we examined whether this inflammatory response might enhance the susceptibility of nearby nerves to VSV injected into the same site. Thus, we modified our approach such that the only CLL-exposed (and hence macrophage-depleted) environment encountered by VSV was the popliteal LN. Because this LN receives lymph from the entire lower leg, we could deplete LN-resident $CD11b^+CD169^+$ macrophages by subcutaneous injection of CLLs into the calf while leaving the footpad unaffected (Fig. 1f and Supplementary Fig. 4a, b). When VSV was injected into essentially normal footpads, mice treated with CLLs in the calf recapitulated the increased mortality observed when both injections were given in the footpad (Fig. 1g). Mice also remained susceptible to neuroinvasion by VSV when they were infected 60 days after injection of CLLs into the footpad (Supplementary Fig. 4c). At this time point, the inflammatory infiltrate in the footpad had resolved, whereas LN macrophages remained depleted (Supplementary Fig. 4d, e)[10]. We conclude that VSV-draining LNs are the principal sites of viral neuroinvasion, and LN macrophages are critical mediators of neuroprotection.

To detect viral replication, we infected macrophage-sufficient mice with VSV–eGFP, which drives green fluorescent protein (GFP) expression selectively within infected cells[11]. Consistent with a recent report[12], VSV replicated selectively in LN macrophages (Fig. 2a, b); however, viral replication was anatomically restricted—only $CD169^{hi}$ SCS macrophages were GFP^+, whereas $CD169^{dim}$ medullary macrophages showed no evidence of viral replication (Fig. 2a and Supplementary Fig. 5). Accordingly, when macrophage-depleted animals were infected with VSV–eGFP, draining LNs were almost completely devoid of GFP^+ cells (Fig. 2c and Supplementary Fig. 5).

To locate peripheral nerves in popliteal LNs, we stained popliteal LNs for β3-tubulin, revealing a branched network of peripheral nerves in the capsule and SCS (Fig. 2d and Supplementary Movies 1 and 2). In VSV–eGFP-infected control animals, these nerves were surrounded by infected (that is, GFP^+) SCS macrophages, but the nerves themselves showed no evidence of VSV replication (Fig. 2e). In contrast, in macrophage-depleted LNs, VSV–eGFP replicated within nerves in and around the SCS. Indeed, the GFP signal co-localized exclusively with β3-tubulin, indicating that VSV replicated selectively in nerves and no other cell types (Fig. 2f, g).

Having established that SCS macrophages protect peripheral nerves against viral neuroinvasion, we investigated three plausible, non-exclusive mechanisms for this vital function: first, that macrophages might phagocytose and destroy viral particles; second, that they might promote adaptive antiviral immune responses; and third, that they might exert innate immune activities thwarting viral entry or replication in nerves. Because SCS macrophages actively replicate VSV (Fig. 2a, b, e), direct macrophage-mediated viral destruction seemed doubtful. Indeed, viral titres were much higher in macrophage-sufficient popliteal LNs than in CLL-treated LNs during the first 36 h after infection (Fig. 2h). Both groups had similarly low viral titres in downstream inguinal LNs (Supplementary Fig. 6a), and VSV was never detectable in the spleen or blood (Supplementary Fig. 6b, c). Thus, the presence of SCS macrophages actually boosted the overall viral burden, presumably by providing a preferred substrate for VSV replication, which is at odds with the idea that these cells prevent viral neuroinvasion by destroying infectious virions.

Previous work had identified SCS macrophages as critical initiators of B-cell activation in LNs[2–4], and humoral immunity is considered essential for VSV clearance[13,14]. However, the neutralizing antibody response in macrophage-depleted mice was not impaired, but rather enhanced in comparison with control animals (Fig. 2i). Similarly, both CD4 and CD8 T-cell responses were normal or even greater in macrophage-depleted mice (Supplementary Fig. 7). Thus, CLL-mediated removal of LN macrophages does not compromise adaptive immunity to peripheral infection with low-dose VSV. In fact, even though SCS macrophages are needed to initiate B-cell activation during the first 6 h after challenge with VSV[2], the overall VSV-specific adaptive immune response was enhanced one week after treatment with CLLs. This may have been due, at least in part, to increased trafficking of antigen-presenting dendritic cells from the inflamed CLL-treated footpad to the draining LN (not shown).

Although CLL-treated mice mounted a supranormal adaptive response to VSV, most nevertheless succumbed to VSV-induced neuropathology (Fig. 1a and Supplementary Fig. 2b, d), indicating that adaptive immunity is insufficient for protection, at least in settings that mimic the natural route and dose of VSV infection. CLL-sensitive LN macrophages apparently make essential contributions to antiviral immunity by one or more innate immune mechanisms. Thus, we investigated the role of IFN-I, which is critical in many viral infections, including VSV[9]. Indeed, on infection with VSV, macrophage-depleted LNs contained about 90% less IFN-α than control LNs did (Fig. 3a).

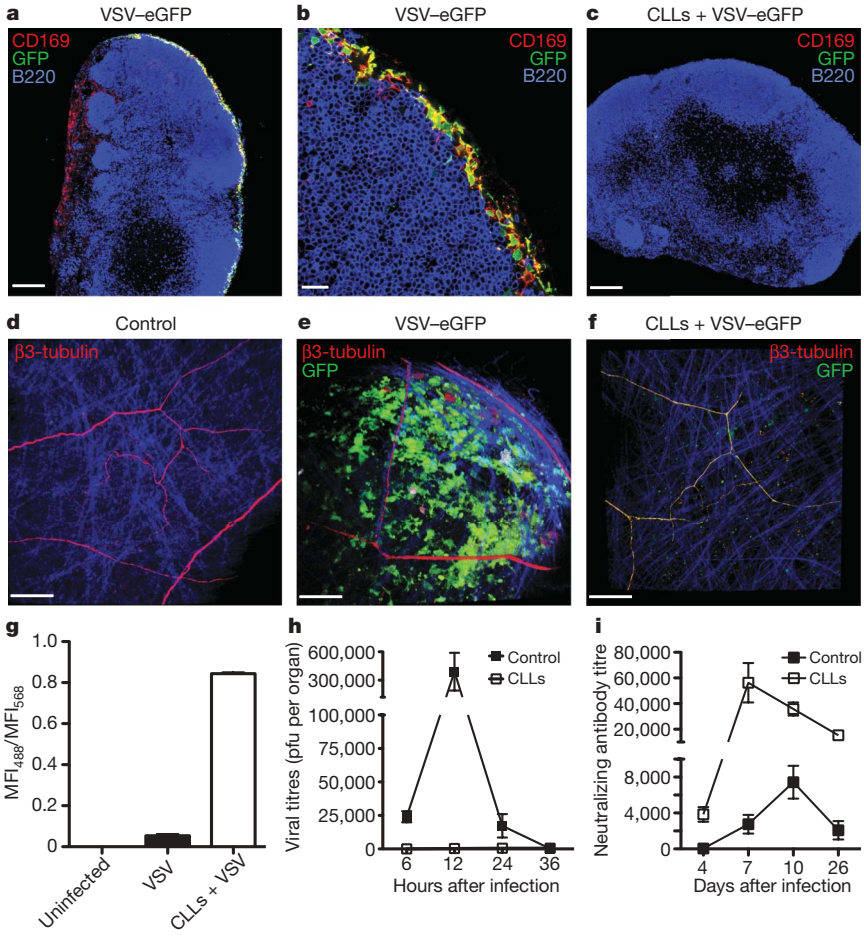

Figure 2 | SCS macrophages are the primary targets for lymph-borne VSV and prevent infection of adjacent nerves. **a**–**c**, Representative confocal micrographs of macrophage-sufficient (**a**, **b**) and CLL-treated (**c**) popliteal LNs after VSV–eGFP infection. Scale bars, 150 μm (**a**, **c**) and 20 μm (**b**). **d**–**f**, Representative multiphoton micrographs of whole mounts of uninfected (**d**) or VSV–eGFP-infected LNs (**e**, **f**). VSV–eGFP infection of macrophage-sufficient LNs (**e**) induced GFP expression in macrophages but not in nerves (red), whereas nerves in CLL-treated LNs (**f**) expressed GFP (Supplementary Movies 1 and 2). Scale bars, 100 μm. Blue shows the second harmonic signal from collagen in the LN capsule. **g**, Ratio of mean fluorescent intensity (MFI) in the green (488 nm) and red (568 nm) channel, depicting GFP expression and β3-tubulin staining, respectively, in peripheral nerves. $n = 3$, $P < 0.0001$ (VSV versus CLLs + VSV). **h**, VSV titres in popliteal LNs of control and CLL-treated mice. $n = 4$, $P = 0.0010$ (6 h), $P < 0.0001$ (12 h), $P = 0.1043$ (24 h), $P = 0.0765$ (36 h). **i**, Serum-neutralizing immunoglobulin titres in control and CLL-treated infected mice. $n = 4$, $P = 0.0053$ (day 4), $P = 0.0138$ (day 7), $P = 0.0022$ (day 10), $P = 0.0054$ (day 26). Error bars show s.e.m.

Accordingly, messenger RNA levels of interferon-inducible genes, such as those encoding 2′,5′-oligoadenylate synthetase (OAS) and interferon-stimulated gene 15 (ISG15), were decreased after macrophage depletion (data not shown).

Next, we examined how macrophage depletion compromised VSV-induced IFN-I production. Conceivably, infected SCS macrophages could produce the cytokine. Alternatively, they could indirectly stimulate IFN-I release by other cells, such as plasmacytoid dendritic cells (pDCs), which recognize VSV through Toll-like receptor (TLR)7 and are a major source of IFN-I in many conditions[15,16]. The number of LN-resident pDCs was not affected by treatment with CLLs (Supplementary Fig. 8a, b) and, unlike SCS macrophages, pDCs were not productively infected by VSV (Supplementary Fig. 8c). However, when pDCs were depleted before VSV infection (Supplementary Fig. 8b), IFN-α levels were 52 ± 0.9% (mean ± s.e.m.) lower than in pDC-sufficient controls (Fig. 3a). Moreover, combined depletion of both pDCs and macrophages abolished IFN-α production (96 ± 0.7% decrease). Thus, whereas pDCs produce IFN-α on subcutaneous infection with VSV, about half of the IFN-I is contributed by CLL-sensitive non-pDCs.

To determine whether VSV induces IFN-I production by SCS macrophages, we infected mice with VSV–eGFP and performed fluorescence-activated cell sorting (FACS) to isolate GFP^+ infected macrophages and GFP^- non-infected LN cells 4 h later (Supplementary Fig. 9a). After culturing equivalent numbers of sorted cells, infected macrophage supernatant contained ~4-fold more IFN-α than non-infected cell supernatant (Fig. 3b). Although the non-infected population contained IFN-α-producing pDCs, the detected IFN-α concentration was low presumably because pDCs are relatively rare among the multitude of other GFP^- cells. Indeed, when we compared GFP^+ SCS macrophages with sorted $CD11c^+GFP^-$ dendritic cells (Supplementary Fig. 9b), the two cell populations produced similar amounts of IFN-α (Fig. 3c). These *in vitro* results fit well with our *in vivo* findings in cell-depleted LNs and establish infected SCS macrophages and pDCs as the two critical sources of VSV-induced IFN-I in peripheral LNs. The relative contributions of other cell types, such as medullary macrophages, to IFN-I production remain to be determined.

CLL-induced macrophage depletion alone decreased IFN-α production almost as efficiently as combined depletion of pDCs and macrophages together (Fig. 3a), suggesting that LN macrophages are required for the production of IFN-I by pDCs. Because pDCs are not infected themselves (Supplementary Fig. 8c), they must localize to LN areas where viral material is accessible for detection by TLR7. Thus, we speculated that macrophages recruit pDCs to the medulla and SCS, where macrophages capture and retain lymph-borne virions[2]. To reveal pDCs, we transplanted mixed bone marrow from wild-type and DPE-GFP × $RAG2^{-/-}$ mice[17] into irradiated wild-type recipients to generate mixed bone-marrow chimaeras in which about 30% of LN pDCs were GFP^+ (Supplementary Fig. 10). In steady-state LNs, most pDCs were located in the T-cell zone with the remainder in the medulla and peri-follicular area (Fig. 3d–i), whereas pDCs were rarely found in the SCS. On infection, pDCs peripheralized from the deep cortex towards the SCS and medulla. However, after macrophage depletion, pDCs in VSV-infected LNs did not depart from the T-cell area and remained scarce in the SCS (Fig. 3g–i and Supplementary Figs 11 and 12). These results indicate that interactions of LN macrophages with VSV lead to pDC relocalization to the site of viral capture and/or infection, presumably as a result of the release of unidentified chemoattractants. Additionally, it is conceivable that virus-exposed macrophages prevent pDC egress into efferent lymph, thus promoting pDC retention in sinus-proximal regions.

In contrast with macrophage depletion, depletion of pDCs with antibodies before VSV infection did not result in increased mortality

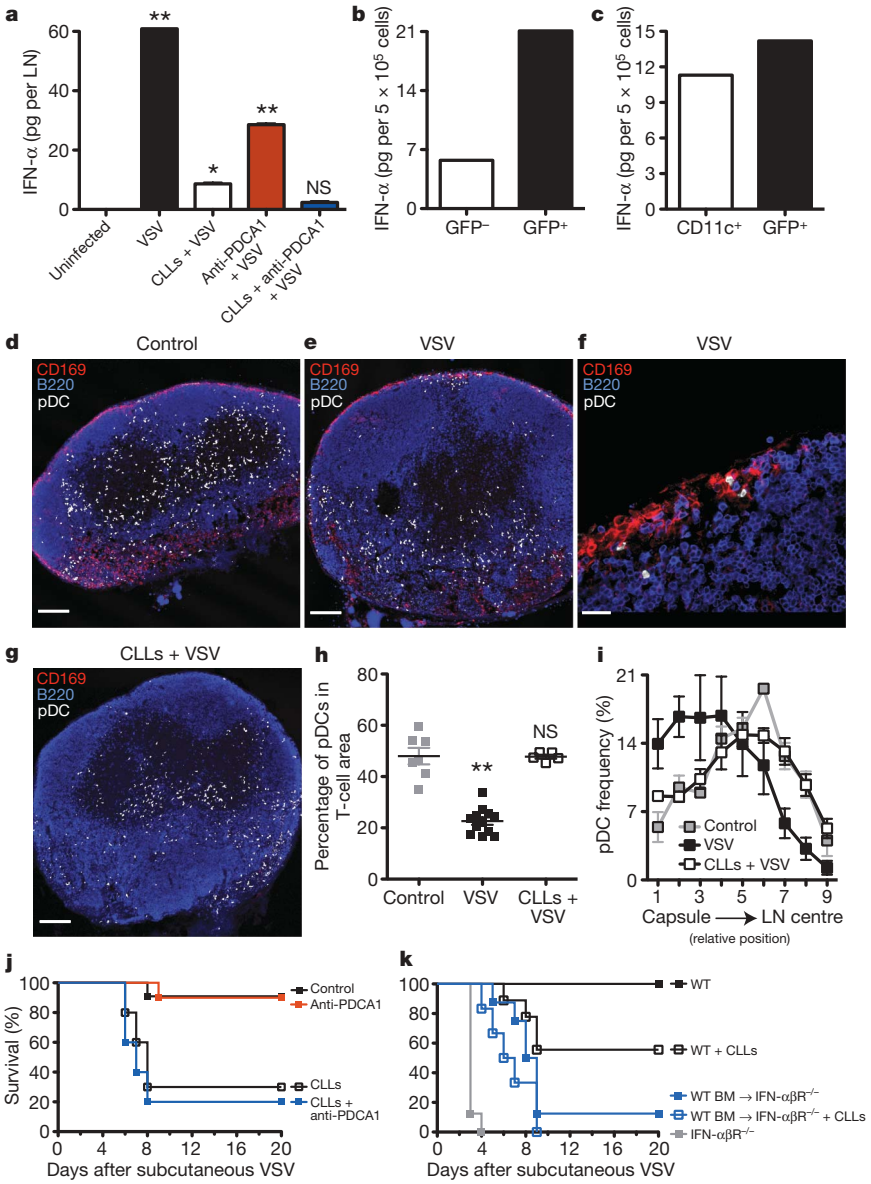

Figure 3 | Regulation of VSV-induced IFN-I production by SCS macrophages. **a**, VSV-induced IFN-α production in LNs ($n = 3$). Asterisk, $P < 0.05$; two asterisks, $P < 0.001$ versus uninfected. NS, not significant. **b**, **c**, IFN-α concentrations in supernatants of FACS-sorted LN cells after VSV–eGFP infection (Supplementary Fig. 9a, b). Results are from one representative experiment of three. **d**–**g**, Micrographs of popliteal LN sections from bone-marrow chimaeric mice with 30% GFP^+ pDCs (Supplementary Fig. 10) that were either left untreated (**d**) or killed 8 h after VSV infection (**e**–**g**) without (**e**, **f**) or with (**g**) pretreatment with CLLs. Scale bars, 150 μm (**d**, **e**, **g**) and 20 μm (**f**). **h**, pDC frequency in the T-cell area ($n = 4$ mice per group). Two asterisks, $P < 0.001$ versus control. **i**, Relative pDC frequency distribution in LN cross-sections (Supplementary Fig. 12). VSV versus control, $P < 0.05$. **j**, Effect of depletion of LN macrophages, pDCs or both on survival on VSV infection; anti-PDCA1 versus control, NS; CLLs versus CLLs + anti-PDCA1, NS. **i**, Survival curves of wild-type (WT), IFN-$\alpha\beta R^{-/-}$ or irradiated IFN-$\alpha\beta R^{-/-}$ mice that were reconstituted with WT bone marrow (BM) on VSV infection. $n = 8$. WT BM→IFN-$\alpha\beta R^{-/-}$ versus WT + CLLs, NS; WT BM→IFN-$\alpha\beta R^{-/-}$ versus IFN-$\alpha\beta R^{-/-}$, $P = 0.0001$. Error bars show s.e.m.

in either control or macrophage-depleted mice (Fig. 3j), suggesting that the localized IFN-I production by SCS macrophages alone is neuroprotective. IFN-I from pDCs seems to be dispensable for survival after VSV infection but may contribute to other aspects of antiviral immunity, such as the development of adaptive responses.

Having determined that macrophage-derived IFN-I is critical, we considered where IFN-I must act to prevent neuroinvasion. We made use of IFN-I receptor-deficient (IFN-$\alpha\beta R^{-/-}$) mice, which are extremely sensitive to VSV infection[9]; after infection with VSV in the footpad, these animals succumbed rapidly within 4–5 days (Fig. 3k) but they did not develop the ascending paralysis observed in CLL-treated wild-type mice. To characterize this difference in disease progression, we generated bone-marrow chimaeras that lacked IFN-αβR in either haematopoietic or non-haematopoietic cells. On subcutaneous infection, mice lacking haematopoietic IFN-αβR recapitulated the phenotype of IFN-$\alpha\beta R^{-/-}$ mice, dying abruptly after 4–5 days without developing ascending paralysis (Supplementary Fig. 13a). By contrast, mice lacking stromal (including peripheral nerve) IFN-αβR showed a slowly ascending CNS pathology, starting with ipsilateral hindlimb paralysis, resembling the disease in macrophage-depleted wild-type mice. Viral replication was always restricted to SCS macrophages when haematopoietic cells expressed IFN-αβR, whereas mice lacking haematopoietic IFN-αβR replicated VSV also in other LN cells (Supplementary Fig. 13b–e). By contrast, macrophage depletion in LNs containing IFN-αβR-sufficient haematopoietic cells did not result in enhanced or aberrant viral replication in LN cells other than peripheral nerves (Fig. 2f, g), indicating that the residual IFN-I produced in CLL-treated wild-type animals is sufficient to protect haematopoietic but not stromal cells.

On the basis of these results, we can reconstruct the chain of events that follows the subcutaneous deposition of VSV: initially, viral particles enter local lymphatics and are transported to draining LNs. Here, two macrophage populations, one in the SCS and the other in the medulla, capture and retain lymph-borne virions[2]. Whereas medullary macrophages do not replicate VSV, SCS macrophages replicate the virus and secrete IFN-I. VSV capture by both macrophage subsets triggers the production of unidentified chemoattractant(s) for pDC, which migrate from the deep cortex towards the SCS and medulla, where they encounter VSV and produce additional IFN-I. A modest amount of macrophage-independent IFN-I is sufficient to protect other haematopoietic LN cells. Higher concentrations and/or localized production of IFN-I are required to prevent viral replication in LN peripheral nerves. Neuroprotective concentrations of IFN-I are achieved only when SCS macrophages are present (and presumably infected by VSV). It remains to be determined whether IFN-I exerts its protective function by preventing viral entry into or replication within peripheral nerves or the

CNS[18], and whether IFN-I acts on neurons or on accessory cells such as Schwann cells. It will be relevant to explore the clinical implications of our findings, particularly for rabies infections and other arthropod-borne neurotropic viruses such as West Nile virus[8].

METHODS SUMMARY

C57BL/6, BALB/c, CD11c-DTR-GFP[19], Tg7 (ref. 20), DPE-GFP[21] and IFN-$\alpha\beta R^{-/-}$ (ref. 9) mice were used. VSV, serotypes Indiana (Mudd-Summers derived clone, *in vitro* rescued[22] and plaque purified), New Jersey (Pringle Isolate, plaque purified) and VSV–eGFP[11] were propagated on BSRT7 cells and purified as described[2]. LN macrophages were depleted by injections of CLLs[23] or diphtheria toxin into the footpad or into the calf 6 days or 60 days before infection. In other experiments pDCs were depleted by intravenous injection of anti-PDCA-1 monoclonal antibody 24 h before infection. VSV titres from organs of infected mice were determined by plaque assay on Vero cells. Serum of infected or control mice was assessed for the presence of neutralizing antibody titres as described[2]. After footpad infection, draining popliteal LNs were harvested for whole-mount immunofluorescence multiphoton microscopy analysis, for flow cytometry analysis, or to generate frozen sections for immunostaining and confocal microscopy. LN protein extracts and supernatants from sorted VSV-infected cells were assayed for IFN-α with an IFN-α enzyme-linked immunosorbent assay (ELISA) kit (PBL InterferonSource). For sciatic nerve resection, the nerve was exposed through an incision on the lateral aspect of the mid-thigh and resected, and the distal and proximal nerve stumps were separately tucked into adjacent intermuscular spaces to prevent nerve regeneration. Results are expressed as means and s.e.m. Means between two groups were compared with a two-tailed *t*-test. Means between three or more groups were compared with a one-way analysis of variance with Bonferroni's post-test. Kaplan–Meier survival curves were compared by using the log-rank (Mantel–Cox) test.

Full Methods and any associated references are available in the online version of the paper at www.nature.com/nature.

Received 1 January; accepted 22 April 2010.

1. von Andrian, U. H. & Mempel, T. R. Homing and cellular traffic in lymph nodes. *Nature Rev. Immunol.* **3,** 867–878 (2003).
2. Junt, T. *et al.* Subcapsular sinus macrophages in lymph nodes clear lymph-borne viruses and present them to antiviral B cells. *Nature* **450,** 110–114 (2007).
3. Phan, T. G., Grigorova, I., Okada, T. & Cyster, J. G. Subcapsular encounter and complement-dependent transport of immune complexes by lymph node B cells. *Nature Immunol.* **8,** 992–1000 (2007).
4. Carrasco, Y. R. & Batista, F. D. B cells acquire particulate antigen in a macrophage-rich area at the boundary between the follicle and the subcapsular sinus of the lymph node. *Immunity* **27,** 160–171 (2007).
5. Lyles, D. S. & Rupprecht, C. E. in *Fields Virology* 5th edn, Vol. 1 (ed. Howley, P. M & Knipe, D. M.) 1363–1408 (Lippincott Williams & Wilkins, 2007).
6. Hangartner, L., Zinkernagel, R. M. & Hengartner, H. Antiviral antibody responses: the two extremes of a wide spectrum. *Nature Rev. Immunol.* **6,** 231–243 (2006).
7. Probst, H. C. *et al.* Histological analysis of CD11c-DTR/GFP mice after *in vivo* depletion of dendritic cells. *Clin. Exp. Immunol.* **141,** 398–404 (2005).
8. Purtha, W. E., Chachu, K. A., Virgin, H. W. & Diamond, M. S. Early B-cell activation after West Nile virus infection requires α/β interferon but not antigen receptor signaling. *J. Virol.* **82,** 10964–10974 (2008).
9. Muller, U. *et al.* Functional role of type I and type II interferons in antiviral defense. *Science* **264,** 1918–1921 (1994).
10. Delemarre, F. G., Kors, N., Kraal, G. & van Rooijen, N. Repopulation of macrophages in popliteal lymph nodes of mice after liposome-mediated depletion. *J. Leukoc. Biol.* **47,** 251–257 (1990).
11. Chandran, K., Sullivan, N. J., Felbor, U., Whelan, S. P. & Cunningham, J. M. Endosomal proteolysis of the Ebola virus glycoprotein is necessary for infection. *Science* **308,** 1643–1645 (2005).
12. Hickman, H. D. *et al.* Direct priming of antiviral $CD8^+$ T cells in the peripheral interfollicular region of lymph nodes. *Nature Immunol.* **9,** 155–165 (2008).
13. Brundler, M. A. *et al.* Immunity to viruses in B cell-deficient mice: influence of antibodies on virus persistence and on T cell memory. *Eur. J. Immunol.* **26,** 2257–2262 (1996).
14. Thomsen, A. R. *et al.* Cooperation of B cells and T cells is required for survival of mice infected with vesicular stomatitis virus. *Int. Immunol.* **9,** 1757–1766 (1997).
15. Asselin-Paturel, C. *et al.* Mouse type I IFN-producing cells are immature APCs with plasmacytoid morphology. *Nature Immunol.* **2,** 1144–1150 (2001).
16. Lund, J. M. *et al.* Recognition of single-stranded RNA viruses by Toll-like receptor 7. *Proc. Natl Acad. Sci. USA* **101,** 5598–5603 (2004).
17. Iparraguirre, A. *et al.* Two distinct activation states of plasmacytoid dendritic cells induced by influenza virus and CpG 1826 oligonucleotide. *J. Leukoc. Biol.* **83,** 610–620 (2008).
18. Detje, C. N. *et al.* Local type I IFN receptor signaling protects against virus spread within the central nervous system. *J. Immunol.* **182,** 2297–2304 (2009).
19. Jung, S. *et al. In vivo* depletion of $CD11c^+$ dendritic cells abrogates priming of $CD8^+$ T cells by exogenous cell-associated antigens. *Immunity* **17,** 211–220 (2002).
20. Maloy, K. J. *et al.* Qualitative and quantitative requirements for $CD4^+$ T cell-mediated antiviral protection. *J. Immunol.* **162,** 2867–2874 (1999).
21. Mempel, T. R. *et al.* Regulatory T cells reversibly suppress cytotoxic T cell function independent of effector differentiation. *Immunity* **25,** 129–141 (2006).
22. Whelan, S. P., Ball, L. A., Barr, J. N. & Wertz, G. T. Efficient recovery of infectious vesicular stomatitis virus entirely from cDNA clones. *Proc. Natl Acad. Sci. USA* **92,** 8388–8392 (1995).
23. Van Rooijen, N. & Sanders, A. Liposome mediated depletion of macrophages: mechanism of action, preparation of liposomes and applications. *J. Immunol. Methods* **174,** 83–93 (1994).

Supplementary Information is linked to the online version of the paper at www.nature.com/nature.

Acknowledgements We thank G. Cheng and M. Flynn for technical support; J. Alton for secretarial assistance; D. Cureton for help and advice with VSV preparations; H. Leung for help with image quantification; R. M. Zinkernagel and H. Hengartner for providing tg7 mice; R. Bronson for help with reading neuropathology; S. Cohen for advice on nerve staining; N. van Rooijen for clodronate liposomes; and the members of the von Andrian laboratory for discussion. This work was supported by National Institutes of Health (NIH) grants AI069259, AI072252, AI078897 and AR42689 (to U.H.v.A.), the Giovanni Armenise-Harvard Foundation (to M.I.) and a NIH T32 Training Grant in Hematology (to E.A.M.).

Author Contributions M.I., E.A.M. and U.H.v.A. designed the study. M.I., E.A.M., E.T., L.B. and T.J. performed experiments. M.I., E.A.M., E.T. and L.B. collected and analysed data. S.P.W. provided reagents and performed the RT–PCR experiment. S.E.H. contributed to the nerve imaging. L.G.G. provided mice and gave conceptual advice. M.I., E.A.M. and U.H.v.A. wrote the manuscript. M.I. and E.A.M contributed equally to this work.

Author Information Reprints and permissions information is available at www.nature.com/reprints. The authors declare no competing financial interests. Readers are welcome to comment on the online version of this article at www.nature.com/nature. Correspondence and requests for materials should be addressed to U.H.v.A. (uva@hms.harvard.edu) or M.I. (Matteo_Iannacone@hms.harvard.edu).

METHODS

Mice. C57BL/6 and BALB/c mice, 6–12 weeks old, were purchased from Taconic Farms, Charles River or the Jackson Laboratory. CD11c-DTR-GFP mice[19] were provided by M. Boes. Tg7 mice[20], expressing an MHC class II ($I\text{-}A^b$)-restricted TCR specific for a peptide derived from the glycoprotein of VSV, were provided by R. Zinkernagel. DPE-GFP mice[21] were bred onto Rag2-deficient background in barrier animal facilities at Harvard Medical School and the Immune Disease Institute (IDI). IFN-$\alpha\beta R^{-/-}$ mice[9] were bred in barrier animal facilities at the Scripps Research Institute. Bone-marrow chimaeras were generated by irradiation of C57BL/6 or IFN-$\alpha\beta R^{-/-}$ mice with 1,300 rad in split doses and reconstitution with C57BL/6, IFN-$\alpha\beta R^{-/-}$ or a 70:30 mix of C57BL/6:DPE-GFP-RAG2KO bone marrow, and were allowed to reconstitute for 8 weeks before use. Mice were housed in specific pathogen-free conditions in accordance with National Institutes of Health guidelines. All experimental animal procedures were approved by the Institutional Animal Committees of Harvard Medical School and IDI, or the Scripps Research Institute.

Viruses. VSV, serotypes Indiana (VSV-IND, Mudd-Summers derived clone, *in vitro* rescued[22] and plaque purified), New Jersey (VSV-NJ, Pringle Isolate, plaque purified) and VSV–eGFP[11] were propagated at a multiplicity of infection of 0.01 on BSRT7 cells, and purified as described[2]. *In vitro*, VSV–eGFP replicates with similar kinetics and endpoint titres to those of the parental recombinant VSV Indiana (data not shown). Infectivity of VSV preparations was quantified by plaque assay on green monkey kidney cells (Vero line), as described[2]. VSV titres from organs of infected mice were determined similarly, after homogenization of the organs with a Potter–Elvehjem homogenizer, as described[2]. Control and macrophage-depleted animals were infected with 10^4 pfu of VSV Indiana into the footpad or intravenously, or with 10^6 pfu of VSV–eGFP into the footpad. All infectious work was performed in designated BL2+ workspaces, in accordance with institutional guidelines, and approved by the Harvard Committee on Microbiological Safety.

***In vivo* depletion of LN macrophages or plasmacytoid dendritic cells.** In some experiments LN macrophages were depleted by subcutaneous injections of 30 µl of CLLs into the footpad or calf, 6 days or 60 days before infection. CLLs were prepared in accordance with a previously published method[23]. In other experiments CD11c-DTR-GFP mice were depleted of LN macrophages by footpad injection of diphtheria toxin (4 ng; Sigma) 6 days before infection. In other experiments pDCs were depleted by an intravenous injection of 500 µg of anti-PDCA-1 depleting antibody (JF05-1C2.4.1; Miltenyi Biotec) 24 h before infection.

Tissue digestion and flow cytometry. Single-cell suspensions of LNs, spleens and footpads were generated by careful mincing of tissues and subsequent digestion at 37 °C for 40 min in DMEM medium (Invitrogen-Gibco) in the presence of 250 µg ml^{-1} liberase CI (Roche) plus 50 µg ml^{-1} DNase-I (Roche). After 20 min of digestion (1 h for footpads), samples were vigorously passed through an 18-gauge needle to ensure complete organ dissociation. All flow cytometric analyses were performed in FACS buffer containing PBS with 2 mM EDTA and 2% FBS (Invitrogen-Gibco) on a FACS CANTO (BD Pharmingen) and analysed with FlowJo software (Treestar Inc.). Antibodies used included allophycocyanin (APC)-conjugated anti-B220 (clone RA3-6B2; BD Pharmingen), APC-conjugated and phycoerythrin (PE)-Cy7-conjugated anti-CD11c (clone HL3; BD Pharmingen), PE-conjugated anti-Ly-6G and Ly-6C (clone RB6-8C5; BD Pharmingen), PE-Cy7-conjugated anti-CD11b (clone M1/70; eBioscience), Alexa Fluor 647-conjugated streptavidin (Invitrogen), PE-Cy7-conjugated streptavidin (BD Pharmingen), Alexa Fluor 647-conjugated anti-F4/80 (clone CI:A3-1; AbD-Serotec), FITC-conjugated anti-CD169 (clone 3D6; AbD-Serotec), biotinylated anti-Vβ2 (clone B20.6; BD Pharmingen), APC-conjugated anti-CD4 (clone L3T4; BD Pharmingen), APC-conjugated anti-CD8 (clone 53-6.7; eBioscience), PE-conjugated anti-IFN-γ (clone XMG1.2; BD Pharmingen), APC-Alexa Fluor 750-conjugated anti-CD45.2 (clone 104; eBioscience), APC-conjugated anti-CD45 (clone 30-F11; BD Pharmingen) and APC-conjugated anti-PDCA1 (clone JF05-1C2.4.1; Miltenyi Biotec). The anti-CD169 antibody Ser4 (provided by P. Crocker) was purified from hybridoma supernatants by standard methods, and biotinylated with a biotinylation kit from Pierce, in accordance with the manufacturer's instructions.

VSV neutralization assay. Serum of infected or control mice was assessed for the presence of neutralizing antibody titres as described[2].

Sorting of VSV-infected cells. Mice were infected in the footpad with 10^6 pfu of VSV–eGFP, and LNs were harvested 4 h later. Twenty infected popliteal LNs were pooled and digested as for FACS (liberase/DNase), and in some experiments stained for CD11c. Cells were sorted on a FACS Aria, and plated in DMEM containing 10% FCS for a further 4 h. Supernatants were collected and stored at −80 °C before being assayed for type I interferon.

Measurement of type I interferon. At 8 h after VSV infection in the footpad, LNs were harvested and homogenized in protein lysis buffer (10 mM Tris-HCl pH 7.4, 150 mM NaCl, 2 mM EDTA, 2 mM EGTA, 1% Triton-X, 0.5% Nonidet P40) in the presence of protease inhibitor cocktail (Roche). LN protein extracts and supernatants from sorted VSV-infected cells were assayed for IFN-α with an IFN-α ELISA kit (PBL InterferonSource), in accordance with the manufacturer's instructions. Total RNA was isolated from frozen LNs as described[24], and analysed for the expression of the IFN-inducible genes encoding OAS and ISG15 by RNase protection assay or by quantitative PCR, as described[24].

Confocal microscopy. Popliteal LNs were harvested, processed, sectioned and stained as described previously[2]. Images were collected with an Olympus Fluoview BX50WI inverted microscope and 10×/0.4 numerical aperture (NA), 20×/0.5 NA or 60×/1.42 NA objectives. Antibodies used included Alexa Fluor 647-conjugated anti-B220 (Clone RA3-6B2; Caltag), biotinylated anti-CD169 antibody (Clone Ser4, see above), Alexa Fluor 568-conjugated streptavidin (Invitrogen) and Alexa Fluor 488-conjugated anti-GFP (Invitrogen). Images were analysed with Volocity software (Improvision) and Photoshop CS3 (Adobe). To assess pDC localization within the LN on VSV infection, we used only selected sections that contained the T-cell area, SCS and medulla. These areas were defined on the basis of staining with B220 and CD169. The number of GFP-expressing pDCs in the T-cell area relative to those present in the SCS and medulla was assessed by manually counting individual GFP-expressing cells. For pDC frequency distribution relative to LN capsule, a perimeter was drawn around each LN section micrograph and subsequently resized by 10% reductions with Microsoft PowerPoint. The number of pDCs located in each concentric ring was counted and plotted as a frequency distribution.

Histological examination of VSV neuropathology. Symptomatic CLL-treated mice and wild-type mice were killed by CO_2 inhalation on day 7–8 after subcutaneous VSV infection. Mice were perfused with and subsequently submerged in Bouin's fixative for 3 days. Tissues were embedded in paraffin, and sagittal and coronal sections of brain and cross-sections of spinal cord were stained with haematoxylin and eosin. Micrographs were made with an Olympus BH-2 light microscope with an Olympus DP71 camera and accompanying DP controller software.

Whole-mount immunofluorescence analysis of popliteal LNs. Popliteal LNs were removed and fixed in phosphate-buffered L-lysine with 1% paraformaldehyde/periodate (PLP). LNs were then washed in PBS containing 1% Triton-X and 0.2% BSA (WM buffer) before being stained overnight with slow agitation at 4 °C. LNs were then washed with frequent changes of WM buffer for 8–12 h, after which the secondary antibodies were added to the WM buffer and incubated again overnight. After 8–12 h of washing on the following day, LNs were analysed on an Olympus confocal microscope (see above) or with a commercial Prairie Technologies Ultima Two Photon Microscope. For two-photon excitation and second harmonic generation, a Tsunami Ti:sapphire laser with a 10-W MilleniaXs pump laser (Spectra-Physics) was used. Antibodies used included anti-neuronal class III β-tubulin (TUJ1; Covance), Alexa Fluor 568-conjugated anti-rabbit IgG (Invitrogen) and Alexa Fluor 488-conjugated anti-GFP (Invitrogen). To assess VSV–eGFP replication in peripheral nerves, the ratio between the mean fluorescent intensity in the green channel (488 nm) and that in the red channel (568 nm) was calculated in selected regions of interest assigned to peripheral nerves (identified by staining with red fluorescent anti-β3-tubulin).

Sciatic nerve resection. Sciatic nerve resection was performed as described previously[25]. In brief, animals were anaesthetized with xylazine (10 mg kg^{-1}) and ketamine HCl (50 mg kg^{-1}), and the sciatic nerve was identified and lifted through an incision on the lateral aspect of the midthigh of the hindlimb. The nerve was then resected and the distal and proximal nerve stumps were separately inserted into nearby intermuscular spaces to prevent nerve regeneration. Subsequently, the incision was closed with a 6-0 non-absorbable running suture (Sofsilk; Tyco Healthcare Group). At 24 h after wound closure, animals were injected into the right footpad with 10^4 pfu of VSV.

Analysis of T-cell responses. For analysis of $CD4^+$ T-cell responses, 10^6 CFSE-labelled tg7 cells were transferred intravenously into recipient mice that were treated or not with CLLs 6 days before infection with 10^4 pfu of VSV. Three days later, single-cell suspensions from the draining popliteal LNs were analysed by FACS, and the number of total tg7 cells or the number of tg7 cells that underwent at least one division was quantified. For the analysis of $CD8^+$ T-cell responses, intracellular IFN-γ staining in the presence or absence of NP52 was performed as described previously[24]. The *in vivo* cytotoxicity assay was performed as described[26].

Statistical analyses. Results are expressed as means and s.e.m. All statistical analyses were performed in Prism (GraphPad Software). Means between two groups were compared by using a two-tailed *t*-test. Means between three or more groups were compared by using a one-way or two-way analysis of variance with Bonferroni's post-test. Kaplan–Meier survival curves were compared by using the log-rank (Mantel–Cox) test.

24. Iannacone, M. *et al.* Platelets mediate cytotoxic T lymphocyte-induced liver damage. *Nature Med.* **11**, 1167–1169 (2005).

25. Shao, C., Liu, M., Wu, X. & Ding, F. Time-dependent expression of myostatin RNA transcript and protein in gastrocnemius muscle of mice after sciatic nerve resection. *Microsurgery* **27,** 487–493 (2007).

26. Iannacone, M. *et al.* Platelets prevent IFN-α/β-induced lethal hemorrhage promoting CTL-dependent clearance of lymphocytic choriomeningitis virus. *Proc. Natl Acad. Sci. USA* **105,** 629–634 (2008).